ISSN 1063-4576, Journal of Superhard Materials, 2020, Vol. 42, No. 4, pp. 264–275. © Allerton Press, Inc., 2020.
Ukrainian Text © The Author(s), 2020, published in Sverkhtverdye Materialy, 2020, Vol. 42, No. 4, pp. 78–92.

INVESTIGATION OF MACHINING PROCESSES

Effect of the Tool Composite Porosity on the Efficiency of Profile Diamond Grinding of Sapphire and Zirconium Dioxide

Ye. O. Pashchenko[a], S. V. Sokhan'[a, *], G. V. Sorochenko[b], D. A. Savchenko[a], O. V. Lazhevska[a], S. V. Skorokhod[a], and O. A. Mikishchenko[a]

[a]*Bakul Institute of Superhard Materials, National Academy of Sciences of Ukraine, Kyiv, 04074 Ukraine*

[b]*Bogomolets National Medical University, Kyiv, 01601 Ukraine*

**e-mail: svsokh@gmail.com*

Received July 24, 2019; revised July 24, 2019; accepted July 25, 2019

Abstract—The efficiency of diamomd grinding of the sapphire and polycrystalline zirconium dioxide spherical surfaces with a diamond tool based on a metal binder with a reduced spread of porous inclusions in size is experimentally investigated. The tool composite is compacted using polyethylene glycol modified with adamantane derivatives, which increases the nonlinearity of the humidifier flow at the stage of briquetting. It is shown that the amplitude of the coefficient of friction decreases by a factor of 3 when such a composite is in friction with zirconium dioxide compared to sapphire friction. In addition, scratches are observed on the polished surface of sapphire in contrast to the case of grinding of zirconium dioxide, to exclude which it is advisable to make sure that the structure of the porous space of the composite has not only a certain size distribution of porous inclusions, but also a reduced value of their most probable size. The parameters of the relative productivity and wear of the diamond tool when grinding sapphire and zirconium dioxide differ by a factor of 2 to 3 depending on the grit size of the abrasive material. The surface roughness of polycrystalline zirconium dioxide upon its fine grinding is generally four to five times lower than that of sapphire.

Keywords: tool composite, distribution of porous inclusions, sapphire, polycrystalline zirconia, spherical surface, precision diamond grinding, porosity structure, surface roughness

DOI: 10.3103/S1063457620040073

INTRODUCTION

At the present stage of development of medical equipment, there is an increased demand for products made of high quality materials, for which the accuracy of manufacture and surface quality are key factors that determine the duration of their service life [1]. Due to the large variety of shapes and sizes of such products, as well as relatively small volumes of production in most cases, high-precision machining centers can perform complex technological transitions and, at the same time, have high flexibility are best suited for their production [2–4]. Diamond grinding is traditionally used to obtain medical products from sapphire and polycrystalline zirconia [4]. In the case of grinding spherical or complex-profile surfaces of ceramic prostheses of heads of joints and other implants made of these intractable materials with an accuracy of ≤1 μm, the problem is to ensure the required surface roughness of the product, which is characterized by parameter $Ra = 0.01–0.02$ μm [5].

Some physical and mechanical properties of sapphire and polycrystalline zirconia made of nanopowders are given in Table 1.

The process of diamond grinding or finishing of products made of any brittle nonmetallic material, in particular, sapphire or polycrystalline zirconia, is radically different from the process of diamond grinding of metals [8, 9]. It is accompanied by elastic/plastic deformation without fracture, dispersion of allowances for plastic deformation, and brittle fracture with splitting off fragments. A characteristic result of removing the allowance during abrasive processing is the lateral chipping and separation of clusters from the surface layer, which manifest themselves in the form of fractures, which have the greatest impact on the formation of surface layer roughness. The probability of certain mechanisms of destruction of the material is determined by both its physical and mechanical properties and the load on the abrasive grains (depending on the treatment modes) [9].

Table 1. Some physical and mechanical properties of sapphire and polycrystalline zirconium dioxide

Parameter	Sapphire (Al_2O_3) [6]	Zirconium dioxide (ZrO_2)* [7]
Density, 10^{-3} kg/m^3	3.99	6.05
Elastic modulus, GPa	400	209
Microhardness H_μ, GPa	19.4–22	10–12
Flexural strength R_{bm}, MPa	>400	850
Critical coefficient K_{Ic} of the intensity of type I stresses, MPa m$^{-1/2}$	3.5	8–11

* The chemical composition of the material is as follows: ZrO_2 (+HfO_2) is the main component; 5.3% Y_2O_3, <0.05% Al_2O_3, <0.01% Fe_2O_3, and <0.02% SiO_2; the contents of the tetragonal and monoclinic phases are 96 and 4%, respectively (Galkin Donetsk Institute of Physics and Technology, National Academy of Sciences of Ukraine, Donetsk, Ukraine).

The microrelief of the formed surface depends, first of all, on the geometrical structure of a working surface of the tool and kinematics of its movement (including the geometry of grains and their distribution in height), fluctuations of the tool with respect to the processed surface (i.e., rigidity of the technological system), elastic and plastic deformations, and brittle fracture in the region of the contact of the tool with the workpiece, and the corrugation and roughness of the working surface of the tool. The random nature of the relief of the grinding wheel is dominant in the formation of roughness due to random location of the grains on the working surface of the wheel. The degree of influence of each of these factors on roughness formation will be different depending on the treatment conditions and physical and mechanical properties of the processed material.

The grinding mode—which depends, in particular, on the value of the normal force applied to the diamond grain—has a main effect on the nature of brittle fracture of nonmetallic material. The destruction due to chipping occurs when the normal force reaches a critical value at which lateral cracks appear. The critical force value at which the formation of lateral cracks occurs can be determined from dependence $P_{cr} = k_P \frac{K_{Ic}^4}{HV^3}$, where k_p is the constant coefficient and HV is the Vickers hardness [10].

Based on the physical and mechanical properties of the materials given in Table 1, the critical force at which lateral cracks are produced in zirconium dioxide is 170 to 200 times greater than the analogous value obtained for sapphire. This means that the critical area of the section of the cut material on the grain, at which scratches appear, has a large value in the case of grinding zirconium dioxide and a plunge depth that is required to form surface scratches in the case of zirconium dioxide is much larger than in the case of sapphire. Therefore, under the same grinding conditions, the number of scratches on the treated surface of zirconium dioxide should be less. On the other hand, critical size l_m of the median crack, at which the scratch begins to develop during indentation, is inversely proportional to the square of brittleness index HV/K_{Ic} of the material in accordance with the following formula [10]: $l_m = \frac{k_m}{\left(HV/K_{Ic}\right)^2}$, where k_m is the constant coefficient. Based on the data given in Table 1, the ratio of these indices for zirconium dioxide and sapphire is 0.2, and the ratio of the median crack critical sizes is 19.7. Experimental studies of the surface layer of zirconium dioxide samples after indentation showed [9] that the value of the half-length of the maximum crack in the surface layer and, consequently, the depth of the layer cracked during diamond machining increase with a decrease in the brittleness index of the material and, consequently, an increase in the critical size of the median crack during indentation.

The current state of studies do not allow us to fully understand the mechanism of formation of the microrelief in such fragile materials as sapphire and polycrystalline zirconia. To ensure the required roughness of the spherical surface of these materials, the diamond tool for fine grinding should steadily maintain the gap in the contact area, which would provide sufficient space to accommodate debris formed during the crumbling of the processed material. It is also important to achieve independence of the flow of debris both on the time and location of the contact spot on the surface of the tool. To meet these conditions, the structure of the tool material must have optimal porosity with a narrow size distribution of porous inclusions. Moreover, tool composites designed for fine grinding must have a sufficiently high wear resistance, which is more characteristic of metal–diamond composites rather than of composites

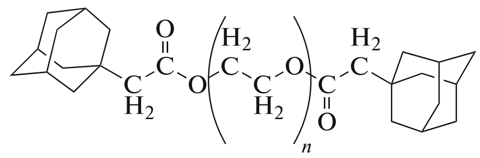

Fig. 1. Fragment of PEG-1500 with bulky hydrophobic groups of adamantane at the ends.

based on polymer binders. Otherwise, the abundant flow of wear products of the binder with a substantial amount of undamaged abrasive grains will not make it possible to achieve uniformly ditributed roughness.

PECULIARITIES OF THE FORMATION OF A POROUS STRUCTURE IN THE TOOL COMPOSITE

The solution to the problem of developing a tool material with specified properties is associated with the manufacture of metal–diamond composites, which would have not only a given porosity, but also a certain structure of the porous space. The compaction of the composite at the initial stage of heat treatment in the mode of warm pressing is a general scheme for the preparation of such a composite. The final stage of heat treatment, which ensures the formation of the required phase composition and mechanical strength of the composite, takes places under conditions of its free sintering.

Under conditions of warm pressing, the technological liquid for humidifying the powder composition plays a decisive role in the formation of the porous structure of the composite. The compaction of a polydisperse ensemble of particles with different shapes is accompanied by their deformation and leads to the formation of numerous channels with variable cross-sectional areas in the system, inside which local flows of the humidifier move. Therefore, the resulting geometric structure of the porous space substantially depends on the mechanism and kinetic parameters of the flow of the organic fluid at the stage of briquetting. Quantitative description of such a flow is complicated, but it is obvious at the qualitative level that this flow depends on such a combination of fluid properties, which can be defined as nonlinearity of rheological behavior. The exponent in the Ostwald–de Ville model can serve as a quantitative measure of the nonlinearity of fluid flow [11–13]. In this study, the degree of nonlinearity of the flow of the humidifier was evaluated at a qualitative level by the experimentally determined dependence of the liquid flow rate on the capillary pressure.

Traditionally, glycerol is used in the manufacture of metal–diamond composites. For example, in the manufacture of tool composites for fine grinding of brittle nonmetallic materials in a powder composition based copper, tin, synthetic diamonds, and a solid lubricant includes a humidifier (glycerol) in the amount of 2 wt %. The mixture is preliminarily briquetted at room temperature with subsequent pressing at a temperature of 553 K.

With the use of glycerol as a high-boiling substance (b.p. 563 K), the spatial distribution pattern of porous inclusions is directly related to the dynamics of fluid redistribution in the process of compacting the components. There was a rather weak dependence of the flow rate of glycerol on the capillary pressure, which indicates a small degree of nonlinearity of the glycerol flow [11]. It should be noted that the use of glycerol leads to materials with a fairly wide distribution of porous inclusions, which is of polymodal nature [11].

It is known that the nonlinearity of rheological characteristics in homologous series of organic oligomers increases with an increase in the molecular weight. Polyethylene glycol (PEG)—which is a similar physicochemical analogue of glycerol—is available in the form of oligomers with different molecular weights. A product with a molecular weight of 1500, which is more than an order of magnitude higher than the molecular weight of glycerol (equal to 97), was chosen for experiments.

Oligomer PEG-1500 was modified by attaching adamantane fragments to obtain a substance that is comprised of fairly long-chain hydrophilic molecules with bulky hydrophobic groups at the ends (Fig. 1).

In the presence of attached terminal hydrophobic bulky functional groups of the adamantane derivative, the nonlinearity of the dependence of the liquid flow rate on the capillary pressure significantly enhances (Fig. 2). The maximum degree of nonlinearity of the system is achieved at 50 mol % of attached adamantane fragments, but the behavior of the system at 553 K again approaches the behavior of glycerol upon increasing their content to 80 mol %. The obtained results correlate with the given size distributions of porous inclusions for metal–diamond compacted composites containing the corresponding products as humidifiers [11]. The largest nonlinearity of the rheological behavior of the humidifier corresponds to

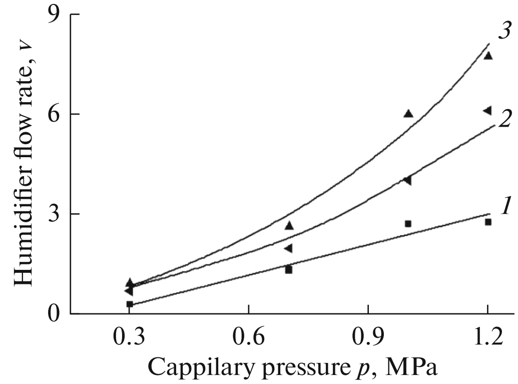

Fig. 2. Dependence of the humidifier flow rate on the capillary pressure for (*1*) glycerol, (*2*) PEG-1500 modified with 30 mol % of adamantane, and (*3*) PEG-1500 modified with 50 mol % of adamantane.

the narrowest size distribution of porous inclusions in the tool compacted composite. In turn, the uniformity of the porous inclusion sizes in fine-grained tool composites has a significant effect on the contact behavior of the latter.

The pycnometric measurements confirm that tool composites sintered in this way have a relatively small (9.6–10%) porosity value with an open system of porous inclusions [12]. The latter circumstance allows one to rather completely describe the size distribution of porous inclusions of composites by the adsorption method [13].

Since the disadvantage of the production of tool composite materials with use of glycerol as a traditional moisturizing additive is associated with the formation of porosity with a fairly wide size distribution of porous inclusions, which is of polymodal nature and leads to a small degree of nonlinearity of the glycerol flow, the use of polyethylene glycol substantially increases the nonlinearity of the dependence of the humidifier flow rate on the capillary pressure and, consequently, reduces the spread of porous inclusions in size. However, the results of previous studies do not allow us to compare the structure of the porous space of the obtained tool composites with the peculiarities of their behavior in dynamic contact with brittle nonmetallic materials during fine grinding of the latter.

The aim of this study was to identify the effect of the porous structure of the tool composite manufactured with use of modified polyethylene glycol on the nature of its interaction with the surface of sapphire and polycrystalline zirconium dioxide, as well as the efficiency of using such a composite in fine diamond grinding of the materials sensitive to damage (the productivity of the grinding process, the wear of the grinding wheel, and the formation of the surface microrelief).

EXPERIMENTAL

The technology of manufacturing metal–diamond tool composites with ASM 7/5 and ASM 3/1 grit sizes for fine grinding of sapphire and polycrystalline zirconium dioxide is proposed for the final formation of porous space at the stage of warm pressing.

One part of the tool composite samples was compacted in the presence of glycerol (see Fig. 2, curve *1*) and the other part was compacted in the presence of PEG-1500 modified with 30 and 50 mol % of adamantane terminal fragments (see Fig. 2, curves *2* and *3*). The grit size of the diamond micropowder in all cases was 3/1.

In the first stage of the study, tool composite samples were tested by paired friction with sapphire and polycrystalline zirconium dioxide. The tests were performed on an II-5018 friction machine according to the pin-on-disk scheme in the air atmosphere at a sliding speed of 0.5 m/s and a pressure of 0.38 MPa.

In the second stage of the study, a ring diamond tool was tested (Fig. 3) using the following method of fine diamond grinding of the spherical sample surfaces. The same grinding scheme that ensured sequential alternation of guiding the rotating tool to plunging and reciprocal-rotational movement of the rotating sample, which provides longitudinal movement of the tool along the treated surface, was used both for the preliminary shaping of the spherical surface and for its finishing (Fig. 4). Precise positioning of the diamond tool relative to the machined surface ensured the achievement of the desired radius of the spherical

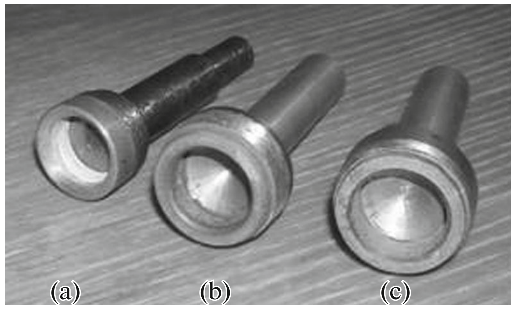

Fig. 3. Ring diamond tools for grinding the spherical sample surfaces with grit sizes of (a) 125/100, (b) 7/5, and (c) 3/1.

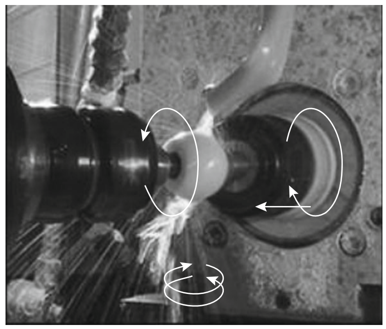

Fig. 4. Diamond grinding of a spherical surface with a mechanism for moving the tool for plunging and reverse rotation of the sample.

surface with high accuracy, while the deviation from the sphericity did not exceed a few fractions of a micrometer.

For fine diamond grinding of spherical sample surfaces with a shape accuracy of ≤1 μm and simultaneously ensuring the surface roughness characterized by parameter Ra = 0.010–0.020 μm, a multipurpose four-axis machining bench designed at the NVO Mikron (Odessa, Ukraine) in accordance with the requirements specified in Technical Assignment for the Bakul' Institute of Superhard Materials, National Academy of Sciences of Ukraine [14]. The bench is made on the basis of a horizontal milling machine with a contouring CNC system and is equipped with a controlled rotating stage on which an additional spindle headstock is arranged (Fig. 5).

For preliminary grinding of spherical surfaces, a ring diamond tool with an outer diameter of 27 mm and an inner diameter of 19 mm and with an inner bevel preformed at an angle of 45° on the working part was used (see Fig. 3a). The tool characteristics were as follows: diamond grinding powder of the AS20 brand with a grit size of 125/100 and a relative concentration of 100; metallic binder of the M2-01 brand. For fine grinding, a ring diamond tool with an outer diameter of 30 mm and an inner diameter of 20 mm without a preformed inner bever was used (the latter was formed with wear of the tool, see Figs. 3b and 3c). The tool characteristics were as follows: ASM diamond micropowders with grit sizes of 7/5 and 3/1 and a relative concentration of 25; experimental metallic binder.

The modes of grinding of spherical surfaces (∅ 28 mm) were characterized by the following parameters: the grinding speed was 4.1–4.7 m/s; the reciprocal-rotational movement of the sample was provided with a rate of 2–3 stroke/min; the rate of guiding the tool to plunging—which depends on the grain size of the tool—was 0.0018–0.01 mm/stroke for sapphire and 0.002–0.03 mm/stroke for zirconium dioxide. A lubricating and cooling technological fluid of the OAK Kool-310 brand, which is typically used in high-precision machining centers, was used as a technological medium. The total thickness of the allowance for the removed layer was 0.10–0.15 mm during pregrinding, 10–30 μm during fine polishing with a diamond tool with a grit size of 7/5, and 3–10 μm during fine polishing with a diamond tool with a grit size of 3/1.

During both preliminary and fine grinding processes, the total allowance layer was removed in several passes with the following technological parameters: 0.01 mm/stroke for sapphire and 0.03 mm/stroke for

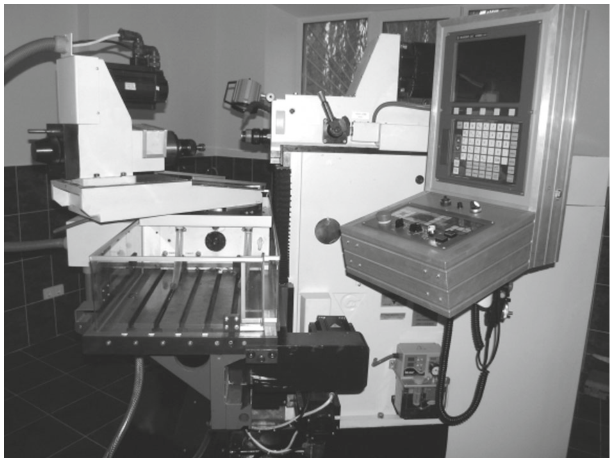

Fig. 5. Experimental multipurpose four-axis bench based on an OMM64SCE02 horizontal milling machine.

zirconium dioxide when guiding the diamond tool with a grit size of 125/100 to plunging; 0.005 mm/stroke for sapphire and 0.008 mm/stroke for zirconium dioxide when guiding the diamond tool with a grit size of 3/1 to plunging; and 0.0018 mm/stroke for sapphire and 0.002 mm/stroke for zirconium dioxide when guiding the diamond tool with a grit size of 7/5. At the end of each pass, idle operation without guiding to plunging was maintained for several strokes. The initial position of the tool at each subsequent pass was set equal to its final position at the previous pass.

For comparative assessment of the quality of treatment of spherical surfaces after fine polishing, it was additionally treated with an ASM diamond paste with agrit size of 1/0 on a cast iron grinder. The following operation modes were used to finish the spherical surface (∅ 28 mm) with a grinder with an outer diameter of ∅ 27 mm and an inner diameter of ∅ 19 mm: the average load on the projection of the grinding region from the force of the clamp was (3.5–3.8) × 10^5 Pa; and the range of fluctuations of the finishing speed in the grinding region was 0.18–1.17 m/s.

Grinding depth ΔR was estimated from a decrease in radius R of the spherical surface, which was measured using a MKTs IP-54-50 digital micrometer with a measuring range of 25–50 mm and an accuracy of 1 μm. Linear wear Δr of the grinding tool in the axial direction was determined indirectly from the results of optical measurement of width b of the made on the tool before and after each pass. The inner bever width values before and after each pass differed by Δb (Fig. 6). The linear wear of the tool in the first pass was not taken into account because of possible lack of contact of the tool with the product at the beginning of the pass.

As can be seen from the diagram given in Fig. 6, the following relations are fulfilled:

$$R^2 = (r_{\text{int}} + b)^2 + (H + \Delta R + \Delta r)^2;$$

$$(R - \Delta R)^2 = H^2 + (r_{\text{int}} + b \pm \Delta b)^2,$$

where H is the current position of the end of the ring tool, which has a hole with radius r_{int}. Knowing the R, ΔR, r_{int}, b, and Δb values, one can easily calculate linear wear Δr of the tool from the above relations. The relative productivity was calculated as a ratio of the linear ($\Delta R/\Delta r$) and volumetric ($\Delta W/\Delta w$) productivity values.

The quality of spherical surface treatment was evaluated using a Mikron-Alpha noncontact interference 3D profilometer based on a MII-4 Linnik microinterferometer (Fig. 7a) by the method described in [15].

Using a Mikron-Alpha profilometer/profilograph, images of the spherical surface of zirconium dioxide and sapphire after fine grinding with a diamond tool with a grit size of 3/1 and after finishing with an ASM diamond paste with a grit size of 1/0 were obtained, as well as the amplitude (*Ra*, *Rq*, *Rp*, *Rv*, *Rt*, and *Rku*), spatial (*Sm*), and functional (*tp*) roughness parameters calculated on the basis of profilograms of the roughness profile with the alignment of the profile curvature according to the results of measurements at a base length of 172 μm averaged over 17 parallel scans of the profile (see Fig. 7b) were quantitatively determined.

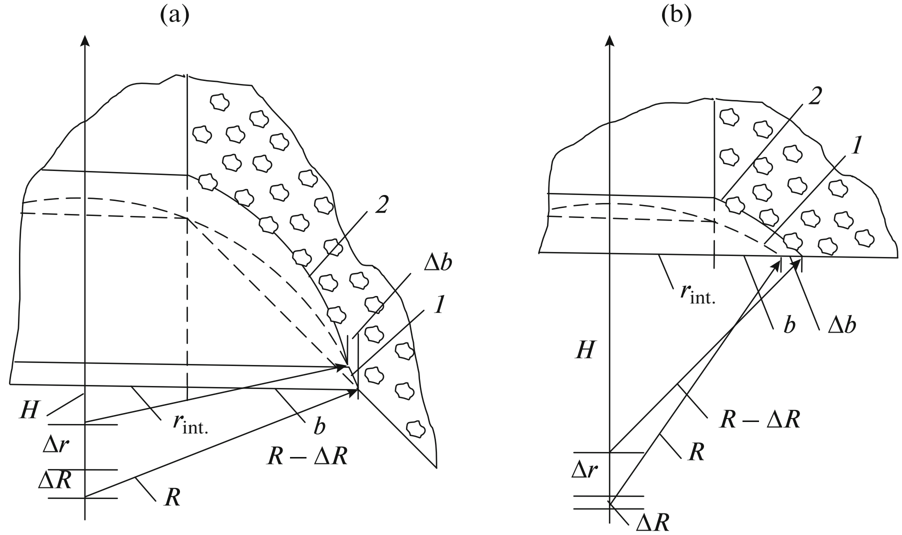

Fig. 6. Scheme for calculating linear wear Δr of the diamond tool in the axial direction in the (a) presence and (b) absence of an internal bevel for the positions of the tool surface (*1*) before and (*2*) after a tool passage.

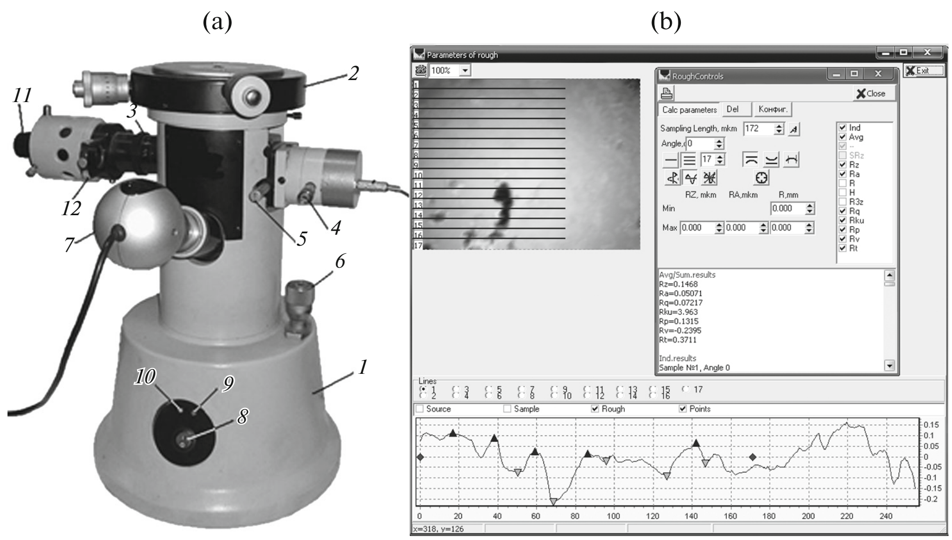

Fig. 7. (a) Mikron-Alpha 3D contactless interference profilometer and (b) its interface.

RESULTS

As a result of testing the friction pairs of the obtained tool composite samples with sapphire and polycrystalline zirconium dioxide samples on an II 5018 friction machine by the disk–cylindrical pin scheme in the air atmosphere at a sliding speed of 0.5 m/s and a pressure of 0.38 MPas, tribograms of the contact interaction of the tool composites with the specified materials are recorded (Fig. 8).

Parameters that characterize the removal of the linear and volume allowances and the wear of the ring diamond tool during preliminary and precision grinding of sapphire and zirconium dioxide are given in Table 2.

In both the processes of preliminary and precision grinding of the spherical surfaces of materials, relative productivity ratio $\Delta R/\Delta r$ barely depends on total plunge depth t in the investigated range of variation of t values (Fig. 9). If this ratio in the case of preliminary grinding of sapphire with a diamond tool with a grit size of 125/100 ranges from 0.72 to 0.78 and is approximately 8% higher than that in the case of preliminary grinding of zirconium dioxide, then this parameter in the case of precision grinding with a dia-

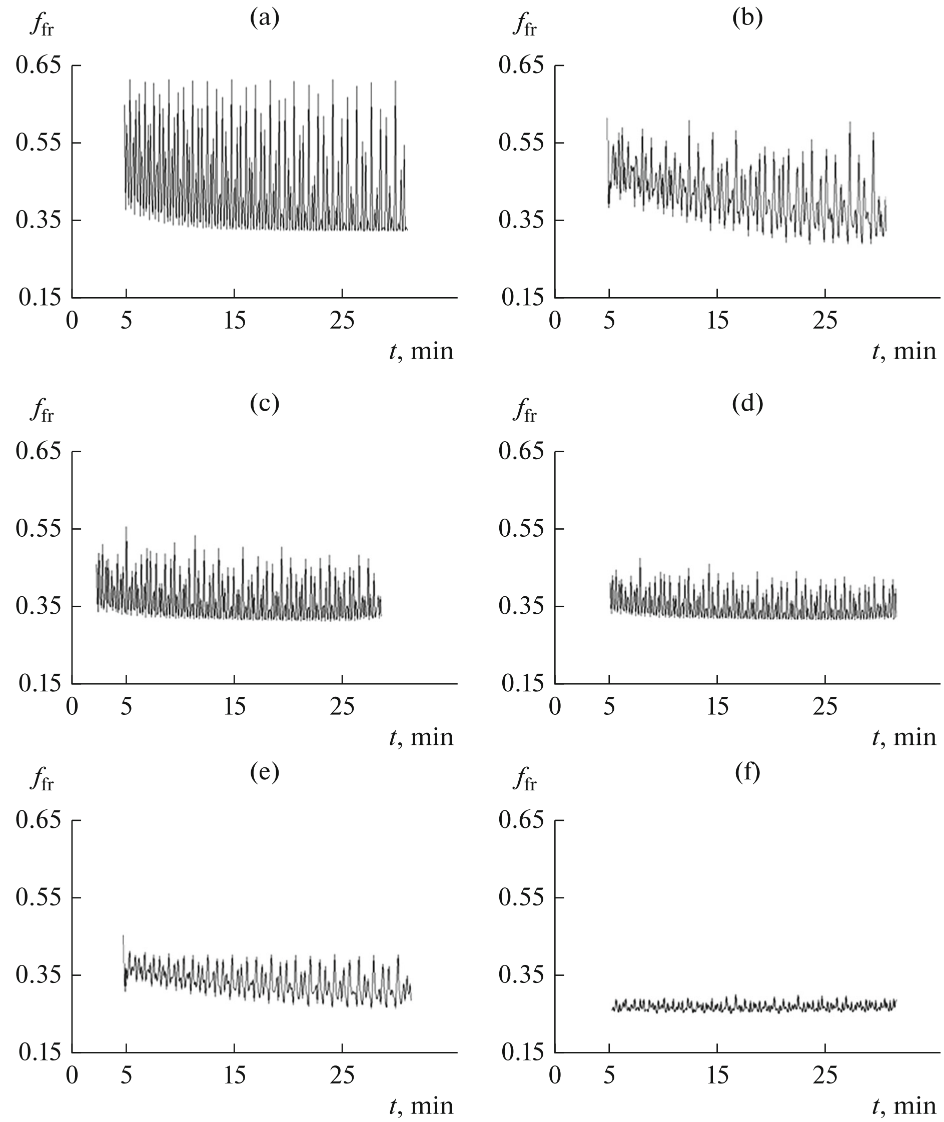

Fig. 8. Tribograms recorded in tests of friction pairs of the tool composite with (a) sapphire and (b) zirconium dioxide, including the composite compacted in the presence of glycerol and PEG-1500 modified with 30 (c and d, respectively) and 50 (e and f, respectively) mol % of terminal adamantane fragments.

mond tool with a grit size of 7/5 is, on the contrary, 19% lower for sapphire compared to zirconium dioxide and ranges from 0.03 to 0.06, just like in the case of precision grinding of both materials with a diamond tool with a grit size of 3/1.

Figures 10–11 show the surface regions of sapphire and zirconium dioxide after grinding with a diamond tool with a grit size of 3/1 and after finishing with an ASM diamond paste with a grit size of 1/0 and the corresponding profilograms of the roughness profile. Profilograms of the sapphire profile are shown for the scan routes with the average step of surface irregularities (*Sm* = 32.9 and 17.9 μm, respectively), which is closest to the average value among the seventeen scan routes specified in Table 3 (see Fig. 7b). Profilograms of the zirconium dioxide profile are shown for the scan route with the average step value of surface irreguliraties (*Sm* = 13.8 and 14.7 μm, respectively), which is closest to the average value among the the seventeen scan routes specified in Table 3.

DISCUSSION

In friction tests, tool composites prepared by using glycerol as a moisturizing additive showed a relatively large amplitude of fluctuations in the coefficient of friction in contact with both sapphire and zir-

Table 2. Parameters of the relative productivity and wear of the diamond tool in the process of grinding of sapphire and zirconium dioxide

Grit size of diamond grinding wheel	Relative productivity of diamond wheel		Relative wear of diamond wheel	
	linear $\Delta R/\Delta r$	volumetric $\Delta W/\Delta w$	linear $\Delta R/\Delta r$	volumetric $\Delta W/\Delta w$
Monocrystalline aluminum oxide (sapphire)				
125/100	0.76	4.52	1.32	0.22
7/5	0.06	0.28	16.67	3.57
3/1	0.03	0.14	33.33	7.14
Polycrystalline zirconium dioxide				
125/100	0.68	4.04	1.47	0.25
7/5	0.19	0.89	5.26	1.12
3/1	0.06	0.28	16.67	3.57

conium dioxide (see Figs. 8a and 8b). We think that this result reflects the nonuniformity of the flow of a slurry suspension that is formed in the operating region, which leads, in turn, to the nonuniformity of the instantaneous distribution pattern of forces. As a result, this nonuniformity leads to the formation of a defective surface layer of the processed materials, i.e., both sapphire and zirconium dioxide. For composites compacted using PEG-1500 modified with 30 mol % of adamantane derivatives, the tribogram amplitudes are also large for both the processed materials (see Figs. 8c and 8d).

However, the tool composite in combination with zirconium dioxide showed a significant decrease in the amplitude of fluctuations in the coefficient of friction with a increase in the degree of modification to 50 mol % (see Fig. 8f), which indicates a much more stable dynamics of removal of the allowance. On the contrary, it was not possible to achieve sufficient improvement of tribological properties in the case of friction pair with sapphire (see Fig. 8e). It seems that sapphire, being a single crystal with sunstantial anisotropy of properties, was too sensitive even to relatively small inhomogeneities in the structure of the pore system of the tool composite. It is also possible that not only the size distribution of porous inclusions is important in this case, but also the value of the most probable pore size which is also needed to be reduced. A further decrease in the size of porous inclusions can be achieved using a wetting additive with a greater degree of nonlinearity of the rheological properties when pressing the composites.

It follows from the obtained results that the productivity of pregrinding of sapphire is approximately 10% higher and the wear of the tool is 10% lower than those values for zirconium dioxide. At the same time, the productivity of fine grinding of zirconium dioxide with a tool with a grit size of 7/5 is approxi-

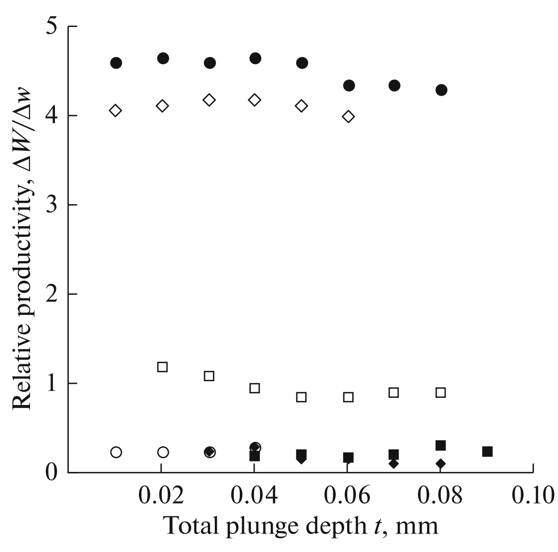

Fig. 9. Dependences of relative productivity $\Delta W/\Delta w$ of grinding (●, ■, ◆) sapphire and (◇, □, ○) zirconium dioxide with diamond tools with grit sizes of (●,◇) 125/100, (■, □) 7/5, and (◆, ○) on the value of total plunge depth t.

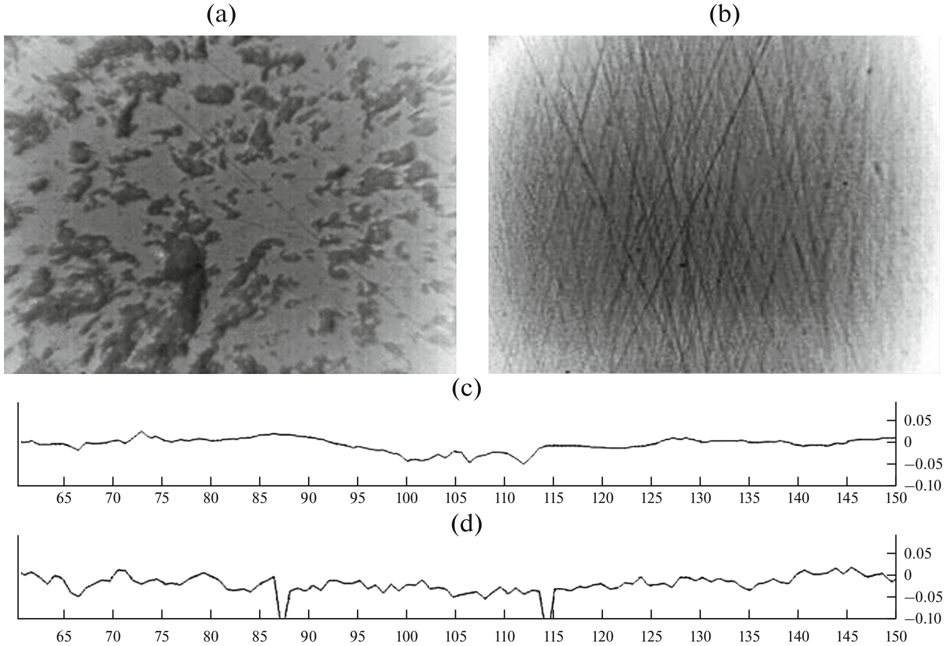

Fig. 10. Images of a surface region of sapphire after (a) fine grinding and (b) finishing, and the profilograms typical of these methods of machining (c and d, respectively).

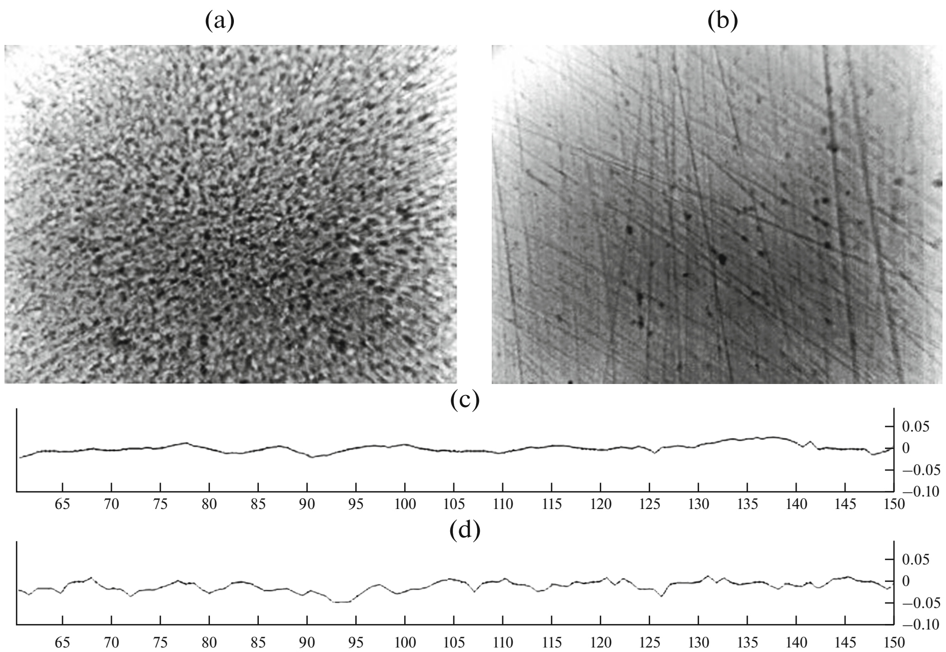

Fig. 11. Images of a surface region of zirconium dioxide after (a) fine grinding and (b) finishing, and the profilograms typical of these methods of machining (c and d, respectively).

mately thrice higher and the wear of the tool is thrice lower than those values for sapphire. When using a tool with a grit size of 3/1, the productivity of grinding of zirconium dioxide is twice higher and the wear of the tool is twice lower than those values for sapphire.

A decrease in the grit size of a diamond tool to 3/1 provides a homogeneous surface of zirconium dioxide without a grid of scratches visible under magnification with a corresponding decrease in the roughness height parameters (see Table 2). Further polishing of the surface with a diamond paste leaves a grid of fin-

Table 3. Height parameters of surface roughness of sapphire and zirconium dioxide after fine grinding and finishing

Roughness parameter	Zirconium dioxide		Sapphire	
	grinding with ASM 3/1 grinding wheel	finishing with ASM 1/0 polishing paste	grinding with ASM 3/1 grinding wheel	finishing with ASM 1/0 polishing paste
Ra, μm	0.0069	0.0073	0.051	0.018
Rq, μm	0.0087	0.0095	0.071	0.022
Rp, μm	0.0223	0.0219	0.136	0.046
Sm, μm	17.8	18.6	34.8	18.0
*tp**, %	55.8	59.4	51.7	61.2
Rt, μm	0.0476	0.0547	0.330	0.092
Rz, μm	0.0381	0.0373	0.142	0.051
Rku	3.192	4.046	5.124	3.063
Rv, μm	0.0253	0.0328	0.194	0.046

* The relative reference length is determined at the midline level.

ishing scratches visible under magnification. The quantitative assessment of the roughness height parameters showed their increase by 5–10% in comparison with fine grinding and a 15% increase in the *Rv* parameter, which indicates a tendency to the formation of a plate-like surface profile in the process of finishing.

The results of visual examination of the sapphire surface after fine grinding with a diamond tool with a grit size of 3/1 indicate the presence of a large number of small punctures with a depth of 0.1–0.3 μm (in some cases, with a depth of 0.4–0.5 μm and even 1.4 μm) which are distributed over the surface against the background of a generally homogeneous microrelief (see Figs. 10c–10e). There are increases in the *Rz*, *Ra*, *Rq*, and *Rt* amplitude parameters of roughness by factors of 1.6–1.7 in places without punctures with a depth of 0.4–0.5 μm and deeper in comparison with the analogous values obtained after fine grinding of zirconium dioxide (see Table 2). The presence of punctures dramatically worsens the roughness (approximately by a factor of 3). Further finishing of the sapphire surface leaves a grid of processing scratches with a depth of no more than 0.02–0.03 μm and provides the complete absence of punctures visible under magnification. However, the value of the amplitude roughness parameters after finishing of the sapphire surface is 1.6–1.7 times higher than the analogous parameters obtained after finishing the zirconium dioxide surface, which indicates poorer quality of machining of sapphire with a diamond tool.

CONCLUSIONS

The use of polyethylene glycol modified with adamantane derivatives in the range of 30–70 mol % in the manufacture of tool composite materials dramatically increases the nonlinearity of the humidifier flow and, accordingly, reduces the size spread of porous inclusions in the composites. The maximum degree of nonlinearity of the system is achieved with a concentration of 50 mol % of grafted adamantane fragments. It is established that the largest nonlinearity of the rheological behavior of the humidifier corresponds to the narrowest size distribution of porous inclusions in the compact. With an increase in the degree of modification to 50 mol %, the tool composite showed a substantial decrease in the amplitude of fluctuations of the friction coefficient in a friction pair with polycrystalline zirconium dioxide, which indicates a much more stable dynamics of removal of the allowance. On the contrary, sufficient improvement of tribological properties cannot be achieved in a friction pair with sapphire. Studies of the microscopic geometry of the surface layers formed in the investigated materials after diamond grinding confirm this conclusion.

Parameters of the relative productivity and wear of the diamond tool in the process of preliminary grinding are approximately identical for both the investigated materials. At the same time, these parameters for the process of fine grinding differ by a factor 2 or 3, depending on the grit size of the diamond tool.

The surface roughness of polycrystalline zirconium dioxide during its fine grinding is generally 4–5 times lower than that of sapphire. Further polishing of the surface with a diamond paste with a grit size of

1/0 leaves a grid of finishing scratches visible under magnification. Quantitative evaluation of the height parameters of surface roughness of zirconium dioxide showed an increase in the surface roughness by about 10% after finishing compared to grinding.

In contrast to polishing of zirconium dioxide, punctures are observed on the polished surface of sapphire, to exclude which one should try to achieve the pore space structure of the composite not only with a certain variation in the size distribution of porous inclusions, but also with a reduced most probable size. Finishing the sapphire surface makes it possible to eliminate chipping and to reduce the surface roughness height parameters by a factor of 3. However, the results achieved by finishing the sapphire surface remain 1.7 times inferior than the results obtained after finishing the surface of zirconium dioxide.

REFERENCES

1. Korzh, M.O., Filipenko, V.A., Tan'kut, V.O., Kosyakov, O.M., Tankut, O.V., and Sokhan', S.V., Modern use of friction pairs in endoprostheses of human joints: Literature review and own research, *Zh. Nats. Akad. Med. Nauk Ukr.*, 2017, vol. 23, nos. 3–4, pp. 247–255.
2. van Iperen, J.-W. and Zanders, R., New strategies for orthopedic machining. https://www.secotools.com/article/83778?language=en.
3. Femoral head machining solutions, Sandvik Coromant. https://www.sandvik.coromant.com/en-gb/industrysolutions/medical/hip/pages/femoral-head.aspx.
4. Müller, A. and Denkena, B., Fine grinding of bioceramics for knee implants with elastically bonded abrasives: process modeling and validation, *J. Ceram. Sci. Technol.*, 2015, vol. 6, no. 1, pp. 31–40.
5. *ISO 7206-2: Implants for Surgery. Partial and Total Hip Joint Prostheses: Articulating Surfaces Made of Metallic, Ceramic and Plastic Materials*. https://www.iso.org/standard/51947.html.
6. Dobrovinskaya, E.R., Litvinov, L.A., and Pishchik, V.V., *Entsiklopediya sapfira* (Encyclopedia of Sapphire), Kharkov: Inst. Monokrist., 2004.
7. Glazunov, F.I., Volkov, G.K., Konstantinova, T.E., Danilenko, I.A., and Glazunova, V.A., Phase stability of ceramics based on the nanopowders ZrO_2–3 mol % Y_2O_3 compacted under high hydrostatic pressure, *Fiz. Tekh. Vys. Davlenii*, 2014, vol. 24, nos. 3–4, pp. 100–110.
8. Filatov, Yu.D., Vetrov, A.G., Sidorko, V.I., Filatov, O.Yu., Kovalev, S.V., Kurilovich, V.D., Danil'chenko, M.A., Prikhna, T.A., Borimskii, A.I., Kutsai, A.M., and Poltoratskii, V.G., Polishing of optoelectronic components made of monocrystalline silicon carbide, *J. Superhard Mater.*, 2015, vol. 37, no. 1, pp. 48–56.
9. Gusev, V.V. and Kalafatova, L.P., *Tekhnologicheskoe obespechenie kachestva obrabotki izdelii iz tekhnicheskoi keramiki* (Technological Support of Product Quality from Technical Ceramics), Donetsk: Donets. Nats. Tekhn. Univ., 2012.
10. Morozov, E.M. and Zernin, M.V., *Kontaktnye zadachi mekhaniki razrusheniya* (Contact Problems of Destruction Mechanics), Moscow: Mashinostroenie, 1999.
11. Minale, M., Modeling the flow of a second order fluid through and over a porous medium using the volume averages. I. The generalized Brinkman's equation, *Phys. Fluids*, 2016, vol. 28, no. 2, pp. 20–35.
12. Walicka, A., Simulation of the flow through porous layers composed of converging-diverging capillary fissures or tubes, *Int. J. Appl. Mech. Eng.*, 2018, vol. 23, no. 1, pp. 161–185.
13. Morhell, N. and Pastoriza, H., Power law fluid viscometry through capillary filling in a closed microchannel, *Sens. Actuators, B*, 2016, vol. 227, pp. 24–28.
14. Rozenberg, O.A., Sokhan', S.V., and Voznyi, V.V., Grinding of sapphire and ceramic implants with precision spherical surfaces, *Instrum. Svit*, 2012, no. 2 (54), pp. 14–21.
15. Sokhan', S.V., Gavlik, I., Nimchevs'ka-Voitsek, M., Efrosinin, D.V., and Mel'nik-Kaglyak, N.A., Evaluation of the roughness of smooth surfaces of nonmetals by the microinterference method, *Zh. Inzh. Nauk*, 2015, vol. 2, no. 2, pp. D1–D9.

Translated by O. Kadkin